

탄소/산화철 나노복합재료의 Brilliant Green 흡착에 대한 반응속도론적, 열역학적 연구

Rais Ahmad* and Rajeev Kumar

Environmental Research Laboratory, Department of Applied Chemistry, Aligarh Muslim University, Aligarh, 202002, India
(접수 2009. 10. 5; 수정 2009. 12. 2; 게재확정 2009. 12. 29)

Kinetic and Thermodynamic Studies of Brilliant Green Adsorption onto Carbon/Iron Oxide Nanocomposite

Rais Ahmad* and Rajeev Kumar

Environmental Research Laboratory, Department of Applied Chemistry, Aligarh Muslim University, Aligarh, 202002, India
(Received October 5, 2009; Revised December 2, 2009; Accepted December 29, 2009)

요약. 본 연구에서는 수용액 중에서 유해한 brilliant green (BG) 제거를 위한 탄소와 산화철 나노복합재료의 흡착특성을 살펴 보았다. 탄소와 산화철 나노복합재료는 화학침전법과 750 °C에서 질산 철과 탄소를 열처리 함으로서 합성하였다. 그 생성물은 TEM, XRD, 그리고 TGA를 이용하여 확인하였다. 나노복합재료에 대한 BG의 흡착 연구는 열역학적 인자와 반응속도론적 인자들을 이용하여 수행하였다. 흡착 속도식은 준 이차 속도식이 준 일차 속도식에 비해 잘 들어맞는다고 보여준다. 실험 결과는 Langmuir 과 Freundlich 흡착 등온선을 이용하여 분석하였다. 평형 데이터는 Langmuir 모델에 잘 들어맞으며 최대 단일 층 흡착 용량 64.1 mg/g 을 갖는다. 열역학적 인자들은 나노복합재료에 BG의 흡착 으로부터 유도하며 흡착은 자발적이며 흡열 과정임을 확인하였다.

주제어: 나노복합재료, 흡착, 열역학, 반응속도론, 탈착

ABSTRACT. In the present work, we have investigated the adsorption efficiency of carbon/iron oxide nanocomposite towards removal of hazardous brilliant green (BG) from aqueous solutions. Carbon/iron oxide nanocomposite was prepared by chemical precipitation and thermal treatment of carbon with ferric nitrate at 750 °C. The resulting material was thoroughly characterized by TEM, XRD and TGA. The adsorption studies of BG onto nanocomposite were performed using kinetic and thermodynamic parameters. The adsorption kinetics shows that pseudo-second-order rate equation was fitted better than pseudo-first-order rate equation. The experimental data were analyzed by the Langmuir and Freundlich adsorption isotherms. Equilibrium data was fitted well to the Langmuir model with maximum monolayer adsorption capacity of 64.1 mg/g. The thermodynamic parameters were also deduced for the adsorption of BG onto nanocomposite and the adsorption was found to be spontaneous and endothermic.

Keywords: Nanocomposite, Adsorption, Kinetic, Thermodynamic, Desorption

INTRODUCTION

Textile industries are using large amount of water and organic chemicals for coloring. Discharging of dyes into water stream even in small amount can affect the aquatic life.¹ The adsorption technique is an effective and attractive process for the treatment of dye-bearing wastewaters. In the literature, clays, zeolites, chitin, bentonite, montmorillonite, fly ash, coconut husk, rice husk, bagasses, apple pomace, sulfonated coal *etc.* were used for the adsorption studies. Increasing use of dyes endangering the environment, encourage the search for low cost and better efficient materials to remove color contaminant from waste water.

The use of nanomaterials as an adsorbent is a new field of interest. Their basic properties like extremely small size and high surface area provide better binding sites for the adsorption of

dyes. More recently, magnetic materials have been employed for the water purification due to easy control and fast separation.²⁻³ It is well known that iron oxides are strong adsorbents for the removal of pollutants such as arsenate, chromates, phosphates, pesticides and humic acids *etc.*⁴ The high adsorption capacity of the iron oxides arise from the hydroxyl groups interaction with the dyes molecules.⁵

In this work, magnetic nanocomposite of carbon/iron oxide was prepared by simple method and their adsorptive characteristic for the removal of brilliant green from aqueous solution was studied. The adsorption studies such as effect of contact time, initial dye concentration, pH and temperature were explored in batch experiments and thermodynamic, kinetic and adsorption isotherm analysis were used to elucidate the adsorption mechanism.

EXPERIMENTAL

Adsorbate

Brilliant green dye (M.F. = $C_{27}H_{34}N_2O_4S$, C.I. = 42040, FW = 462.65, λ_{max} = 625 nm), supplied by CDH New Delhi, India was used as an adsorbate. BG molecules exists as cation in aqueous medium.

Preparation of carbon/iron oxide nanocomposite

Carbon was prepared from ginger (*Zingiber officinale*) waste rhizome in muffle furnace at 600 °C. Carbon was then extensively washed with double distilled water and dried at 450 °C. The composite was prepared from a suspension of carbon (5 gm) in 15 mL aqueous solution of ferric nitrate (5 gm) and NaOH (10 mL of 10 M) was then added drop wise to precipitate the iron oxide. The precipitated material was agitated at 30 °C for 6 h, filtered and calcined at 750 °C for 1 h. The resulting material was then thoroughly washed with double distilled water, dried at 60 °C and used as such for adsorption studies.

Characterization

The morphology of nanocomposite was obtained using transmission electron microscopy (Philips TEM 420). Thermogravimetric analysis was performed by (DTG-60H, Shimadzu) in the presence of nitrogen at the flow rate 30 mL min⁻¹. The crystal structure of the particles was characterized by Philips X'Pert PRO X-ray diffraction system.

Adsorption and desorption studies

Adsorption studies of carbon/iron oxide nanocomposite were performed in batch for the removal of BG from aqueous solution. For kinetic study, 20 mL of dye solution of known concentration was poured into 100 mL flask with a fixed amount (0.02 g) of nanocomposite and was shaken at different time intervals. To obtain the equilibrium isotherms, initial concentration of BG was varied from 10 - 50 mg/L while keeping the adsorbents dose (0.02 g), pH (6.2) and contact time constant. The effect of initial pH on BG adsorption was investigated by varying the initial pH of the dye solution from 5.0 - 9.0 because of the fact that below the pH 5.0 iron oxide starts getting dissolve in the acidic solution⁶ and above pH 9.0, BG shows color change. The initial pH values of the solution were adjusted with diluted HCl and NaOH. The amount left in solution after adsorption was determined by the UV-visible (Elico SL-164 model) double bean spectrophotometer at 625 nm. The extent of dye removal was calculated as follows

$$q_e = (C_i - C_f)V/m \quad (1)$$

where q_e is the adsorption capacity ($mg\ g^{-1}$), C_i and C_f are the initial and final concentrations ($mg\ l^{-1}$) of dye in the solution,

m is the mass of adsorbent (g) and V is the volume of solution (l).

Desorption of BG was studied by placing 0.02 g dye saturated adsorbent into 20 mL acetic acid (0.1 and 1 M) for 3 hrs contact time and the amount of dye desorbed was analysed spectrophotometrically.

RESULT AND DISCUSSION

Characterization

The morphology of nanocomposite was characterized by TEM. Fig. 1 shows that the particles are spherical in shape and size varies from 46 - 59 nm.

Fig. 2 illustrate the X-ray diffractogram of nanocomposite in the 2θ range of 5 - 80°. Six narrow peaks at 2θ values of 29.40, 31.90, 38.90, 42.5, 47.90 and 48.38 indicate that nanocomposite is crystalline in nature. The crystallite sizes were calculated using the Scherrer's equation:

$$D = k \lambda / \beta \cos \theta \quad (2)$$

where k is a constant ~ 0.9 , λ is the wavelength of X-rays, β is the full width of diffraction peak at half maximum intensity and θ is the Bragg's angle. The calculated crystallite sizes were

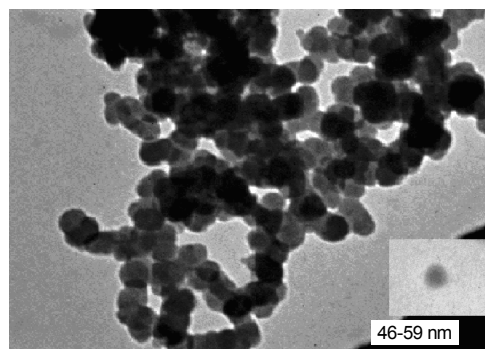


Fig. 1. TEM image of carbon/iron oxide nanocomposite at 18 K.

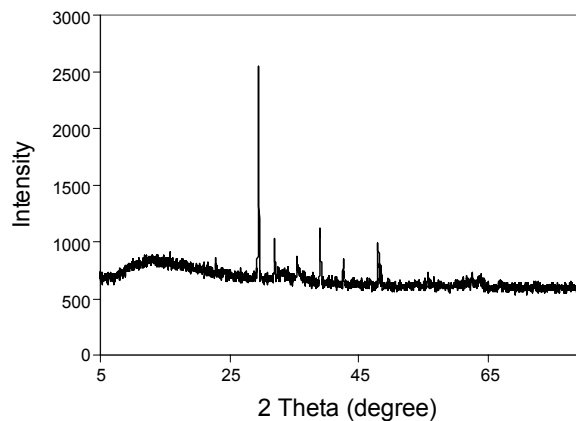


Fig. 2. XRD pattern of carbon/iron oxide nanocomposite.

found to be in the range of 10.2 - 15.9 nm. The crystallinity of the composite was originated due to the iron oxide because it is well known that carbon is amorphous in nature.

TEM showed the larger particle size than XRD. This may be due to the fact that the particle size given by XRD corresponds to the average of the smallest undistorted regions in the nanocomposite, whereas TEM counting is related to regions separated by more-or-less sharp contours in the TEM micrograph. Therefore, when dislocations are arranged in a configuration, which causes small orientation differences between two adjacent regions, the XRD size corresponds to the two separate regions, whereas in the TEM micrograph the two regions may seem to correspond to the same particle.⁷⁻⁸

Fig. 3 shows the thermogravimetric analysis of the carbon/iron oxide nanocomposite. The first weight loss is due to the moisture while the second weight loss is related to the oxidation of carbon. As the thermo analysis temperature increase, the Fe atom oxidizes.⁹

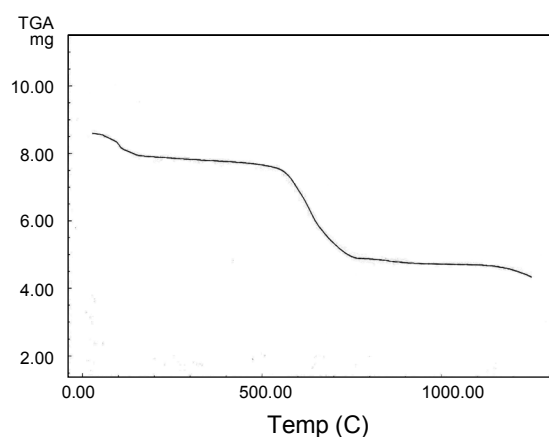


Fig. 3. TGA curve of carbon/iron oxide nanocomposite.

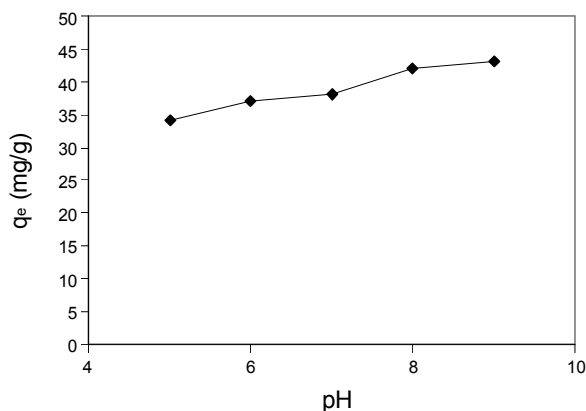
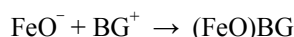
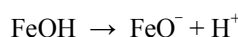


Fig. 4. Effect of initial solution pH on BG adsorption (dye conc.: 20 mg/L, adsorbent dose: 0.02 g, temp.: 30 °C).

The approximate amount of iron oxide in the composites was calculated by subtracting the residual weight of the blank carbon from residual weight of composite at 1120 °C. It was observed that the estimated weight percent of iron oxide is 31%.

Effect of initial solution pH

Adsorption of BG onto nanocomposite was influenced by pH of the solution. The results as depicted in Fig. 4 shows that dye removal increases with increasing initial pH of the dye solution and maximum removal was found to be at pH 9.0. The adsorption mechanism under the influence of initial solution pH may be explained with respect to the carbon and iron oxide. The most abundant surface functional group participating in the adsorption on adsorbent is the hydroxyl group, which is amphoteric and reactive.³ The hydroxyl group may undergo deprotonation in basic condition and get negative charge, which make the adsorption favorable due to electrostatic interaction between cationic BG dye (BG⁺) and anionic iron oxide. Therefore, the following reactions were expected to occur at the iron oxide/liquid interface in basic medium:



and the adsorption onto carbon probably due to the presence of excess OH⁻ groups on the adsorbent surface, which enhance the electrostatic interaction between cationic dye and negatively charged adsorbent surface. Therefore, C-OH + BG⁺ → (C-OH)BG, reaction was expected to occur at the carbon/liquid interface in basic medium.

Effect of contact time and kinetics

Adsorption of BG increases with increase in contact time (Fig. 5) and reaches the equilibrium within 120 min, indicating high affinity of dye molecules for nanocomposite. The rate of BG removal was very rapid initially (exterior surface). After that dye molecules entered into the pores of nanocomposite and were adsorbed by the interior surface, which takes relatively long time.¹⁰

Lagergren pseudo-first¹¹ and Ho's pseudo-second-order rate¹² equations were used to describe the BG adsorption kinetics. Pseudo-first and pseudo-second-order rate equations are presented in equations (3) and (4), respectively

$$\log (q_e - q_t) = \log q_e - k_1 t / 2.303 \quad (3)$$

$$t/q_t = 1/k_2 q_e^2 + t/q_e \quad (4)$$

where q_e and q_t are the amount of dye adsorbed (mg g⁻¹) at

equilibrium and at time t (min). k_1 and k_2 are the pseudo-first and pseudo-second-order rate constants, respectively. The q_e , k_1 and k_2 values could be determined from the slope and intercept of their respective plots of $\log (q_e - q_t)$ vs t and t/q_t vs t .

Linear equations of pseudo-first and pseudo-second-order rate kinetics, based on experimental data in Fig. 5 were presented as:

$$\log (q_e - q_t) = 1.397 - 0.0133 t, R^2 = 0.8055 \quad (5)$$

$$t/q_t = 0.363 + 0.024 t, R^2 = 0.9948 \quad (6)$$

The high value of correlation coefficient for pseudo-second-order equation shows that adsorption of BG is following pseudo-second-order kinetic model.

In order to identify the rate of adsorption process and ascertaining that whether the on-going process is particle diffusion or film diffusion, the applicability of film diffusion model was studied.

$$\ln (1 - F) = -K_f t \quad (7)$$

where F is the fraction attainment of equilibrium. K_f is the film diffusion rate constant (min^{-1}). To find the actual process involved, time vs $\ln (1 - F)$ was plotted (Fig. 6), and a straight line deviating from origin was obtained, which suggests the film diffusion as rate determining step.¹³

Effect of dye concentration

The influence of BG concentration on dye adsorption was presented in Fig. 7. When the BG concentration was increased from 10 to 50 mg/L, dye adsorption onto carbon/iron oxide increased from 24 to 48 mg/g.

The adsorption isotherm describes how adsorbate molecules interact with adsorbents when the adsorption process approaches to an equilibrium state. Equilibrium adsorption isotherm data were analyzed according to Langmuir and Freundlich models. The linear Langmuir and Freundlich equation were, respectively, described as:

$$C_e/q_e = C_e/Q_e + 1/b Q_e \quad (8)$$

$$\log q_e = \log K_f + 1/n \log C_e \quad (9)$$

where C_e is the equilibrium concentration of the dye solution (mg l^{-1}), q_e is the amount of dye adsorbed at equilibrium (mg g^{-1}), Q_e is the calculated maximum monolayer adsorption capacity (mg g^{-1}) and b is Langmuir constant. K_f and n are Freundlich constants indicating adsorption capacity and intensity, respectively. The values of Langmuir and Freundlich parameters were calculated from the slope and intercept of linear plots of C_e/q_e vs C_e and $\log q_e$ vs $\log C_e$, respectively.

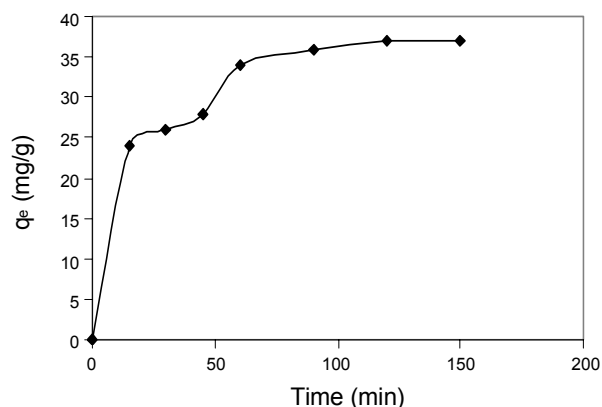


Fig. 5. Effect of contact time on BG adsorption (dye concentration- 20 mg/L, adsorbent dose- 0.02 g, temp.- 30 °C).

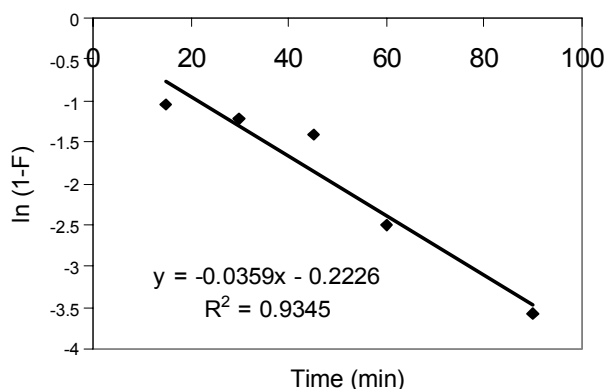


Fig. 6. Time vs $\ln (1 - F)$ graph for BG adsorption.

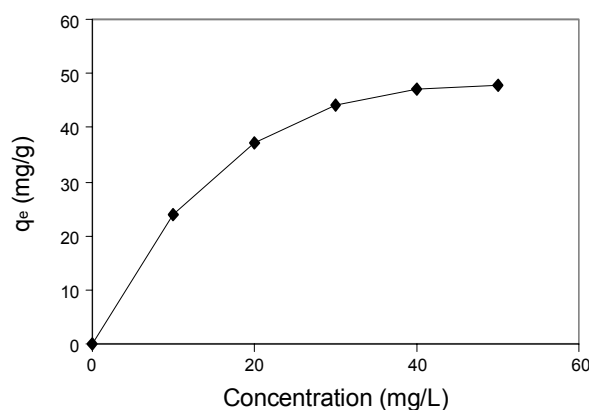


Fig. 7. Effect of BG concentration on its adsorption (adsorbent dose: 0.02 g, pH: 5.6, temp.: 30 °C).

Langmuir and Freundlich equations based on the experimental data in Fig. 7, can be presented as:

$$C_e/q_e = 0.0156C_e + 0.0655, R^2 = 0.9925 \quad (10)$$

$$\log q_e = 0.9649 + 0.4407 \log C_e, R^2 = 0.9468 \quad (11)$$

Table 1. Comparison of maximum monolayer adsorption capacity for the BG onto various adsorbents

Adsorbent	Q _e (mg g ⁻¹)	Reference
Chemical activated carbon	286	[14]
Steam activated carbon	150	[14]
Charcoal	52	[14]
Acid treated almond peel	123.41	[15]
Fly ash	116.28	[16]
Kaolin	65.42	[17]
Rice husk ash	25.13	[18]
Jalshakti	17.6	[19]
Carbon/iron oxide nanocomposite	64.10	this study

Table 2. Thermodynamic parameters for BG adsorption

ΔG ⁰ (kJ mol ⁻¹)			ΔH ⁰ (kJ mol ⁻¹)	ΔS ⁰ (J mol ⁻¹ K ⁻¹)
298 K	303 K	308 K		
-2.980	-5.214	-7.669	124.152	6.178

It was found that the correlation coefficient of Langmuir and Freundlich isotherms were 0.9925 and 0.9468. This revealed the data were better fitted to the Langmuir equation than Freundlich equation. The maximum monolayer adsorption capacity (Q_e) of nanocomposite for BG was found to be 64.10 mg g⁻¹. The Comparison of maximum monolayer adsorption capacity for the BG onto various adsorbents is shown in Table 1.

Effect of temperature and thermodynamics

The adsorption of BG was found to increase from 28 to 38 mg g⁻¹ when the temperature was increased from 298 to 308 K. The enhancement in the adsorption capacity may be due to the decrease in viscosity of solution and increase in rate of diffusion of adsorbate molecules in the internal pores of adsorbent particles.²⁰

Thermodynamic studies were performed, to find the nature of adsorption process. Thermodynamics parameters i.e. free energy (ΔG⁰), enthalpy (ΔH⁰) and entropy (ΔS⁰) were calculated using Van't Hoff and Gibb's-Helmholtz equations:

$$\Delta G^0 = -RT \ln K_c \quad (12)$$

$$K_c = C_{ae}/C_e \quad (13)$$

$$\ln K_c = \Delta S^0/R - \Delta H^0/RT \quad (14)$$

where C_{ae} and C_e are the equilibrium concentration of dye (mg g⁻¹) on the adsorbent and solution, respectively. K_c is the equilibrium constant, T is the solution temperature (K) and R is the gas constant.

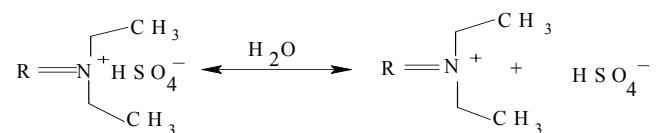
The negative ΔG⁰ values indicate the feasibility and spontaneity of the adsorption process (Table 2). The positive value of ΔH⁰ suggests the endothermic nature of adsorption. The positive value of ΔS⁰ shows the increase in randomness at solid/solution interface and entropically favorable adsorption of BG.

DESORPTION

In order to investigate the regeneration capacity, sodium hydroxide, water and acetic acid were used for desorption from BG saturated adsorbent. NaOH (1 M) and water did not show any desorption of BG. But 0.1 and 1 M CH₃COOH solubilised 58 and 80% of dye. The dye molecules attached on the adsorbent surface easily desorbs in 0.1 M CH₃COOH but at high concentration, CH₃COOH (1M) get diffuse into pores of the adsorbents and as a result, solubility of dye increases.²¹

ADSORPTION MECHANISM

Adsorption of BG may take place by either chemisorption or physisorption or both. There are many factors that may influence the adsorption behavior, such as dye structure and size, adsorbent surface properties, steric effect and hydrogen bonding *etc.* BG is a cationic dye. In aqueous solution, it dissociate as:



where R is used for the rest of the dye molecule.

The interactions between BG and composite surface can be divided into weak and strong interactions. The weak interaction occurs due to the presence of van der Waals forces, while strong interaction occurs due to (a) the hydrogen bonding between the oxygen and nitrogen containing functional groups of dye molecules and adsorbent (b) hydrophobic-hydrophobic interactions between the hydrophobic part of BG molecules and adsorbent. Under the influence of dye solution pH, the adsorption may take place by electrostatic force which was discussed earlier (Effect of initial solution pH).

CONCLUSION

The present study confirmed that carbon/iron oxide nanocomposite is a promising adsorbent for the removal of BG from aqueous solution. The maximum adsorption was attained within 120 min. The optimum pH for the adsorption of BG was found to be at 9.0 and an electrostatic attraction was observed between negatively charged adsorbent at pH > 7.0 with positively charged

ed dye molecules. The equilibrium data fitted well in the Langmuir model of adsorption, showing monolayer coverage of dye molecules at the outer surface of nanocomposite. Adsorption of BG increases with increase in temperature, indicating endothermic nature of adsorption following pseudo second order kinetic.

REFERENCES

1. Bhatnagar, A.; Jain, A. K.; Mukul, M. K. *Environ. Chem. Lett.* **2005**, *2*, 199.
2. Chang, C. F.; Lin, P. H.; Hall, W. *Colloid. Surface. A. Physicochem. Eng. Asp.* **2006**, *280*, 194.
3. Banerjee, S. S.; Chen, D. H. *J. hazard. Mater.* **2007**, *147*, 792.
4. Stipp, S. L. S.; Hansen, M.; Kristensen, R.; Hochella, M. F.; Benned- sen, L.; Diderikesen, K.; Balic, Z. T.; Leonard, D.; Mathieu, H. J. *Chem. Geol.* **2002**, *190*, 321.
5. Pirillo, S.; Ferreira, M. L.; Rueda, E. H. *Ind. Eng. Chem. Res.* **2007**, *46*, 8255.
6. Oliveira, L. C. A.; Rios, R. V. R. A.; Fabris, J. D.; Garg, V.; Sapag, K.; Lago, R. M. *Carbon* **2002**, *40*, 2177.
7. Ungar, T. *J. Mater. Sci.* **2007**, *42*, 1584.
8. Zhong, Y.; Ping, D.; Song, X.; Yin, F. *J. Alloy. Comp.* **2009**, *476*, 113.
9. Pomogailo, A. D.; Dzhardimalieva, G. I.; Rozinberg, A. S.; Mura- viev, D. M. *J. Nanopart. Res.* **2003**, *4*, 497.
10. Anirudhan, T. S.; Divya, L.; Suchithra, P. S. *J. Envir. Manag.* **2009**, *90*, 549.
11. Lagergren, S. K. *Svenska Vetenskapsad Handl.* **1898**, *24*, 1.
12. Ho, Y. S. *Ph. D. thesis, University of Birmingham, Birmingham, U. K.* **1995**.
13. Mittal, A. *J. hazard. Mater.* **2006**, *133*, 196.
14. Asadullah, M.; Asaduzzaman, M.; Kabir, M. S.; Mostofa, M. G.; Miyazawa T. *J. hazard. Mater.* **2010**, *174*, 437.
15. Ahmad, R.; Mondal P. K. *Sep. Sci. Tech.* **2009**, *44*, 638.
16. Mane, V. S.; Mall, I. D.; Srivastava, V. C. *Dyes Pigm.* **2007b**, *73*, 269.
17. Nandi, B. K.; Goswami, A.; Purkait, M. K. *J. hazard. Mater.* **2009**, *161*, 387.
18. Mane, V. S.; Mall, I. D.; Srivastava, V. C. *J. Environ. Manage.* **2007**, *84*, 390.
19. Dhodapkar, R.; Rao, N. N.; Pande, S. P.; Nandy, T.; Devotta, S. *React. Funct. Poly.* **2007**, *67*, 540.
20. Wang, S.; Zhu, Z. H.; *Dyes. Pig.* **2007**, *75*, 306.
21. Inbaraj, B. S.; Sulochana, N.; *Ind. J. chem. Tech.* **2006**, *1*, 17.